J Breast Cancer. 2020 Aug;23(4):355-372
https://doi.org/10.4048/jbc.2020.23.e47
pISSN 1738-6756·eISSN 2092-9900

Journal of Breast Cancer JBC

Original Article

MiR-183-5p Promotes Proliferation, Metastasis and Angiogenesis in Breast Cancer Cells through Negatively Regulating Four and a Half LIM Protein 1

Yi Li [1,2,*], **Qing'an Zeng** [1,*], **Jiliang Qiu** [3], **Ting Pang** [4], **Fenglian Ye**[1], **Lin Huang** [1], **Xuexia Zhang** [2,5]

[1]Department of Thyroid & Breast Surgery, The Fifth Affiliated Hospital, Sun Yat-sen University, Guangzhou, China
[2]Guangdong Provincial Key Laboratory of Biomedical Imaging, The Fifth Affiliated Hospital, Sun Yat-sen University, Guangzhou, China
[3]Department of Surgery, Sun Yat-sen University Cancer Center, State Key Laboratory of Oncology in South China, Collaborative Innovation Center for Cancer Medicine, Guangzhou, China
[4]Department of Anesthesiology, The Sixth Affiliated Hospital, Sun Yat-sen University, Guangzhou, China
[5]Department of Anesthesiology, The Fifth Affiliated Hospital, Sun Yat-sen University, Guangzhou, China

Received: Mar 13, 2020
Accepted: Aug 17, 2020

Correspondence to
Xuexia Zhang
Department of Anesthesiology and Guangdong Provincial Key Laboratory of Biomedical Imaging, The Fifth Affiliated Hospital, Sun Yat-sen University, No. 52 Meihua East Road, Xiangzhou District, Zhuhai, Guangdong Province 519000, China.
E-mail: liyi8@sysu.edu.cn

*These authors contributed equally to this work.

ORCID iDs
Yi Li
https://orcid.org/0000-0001-9717-1719
Qing'an Zeng
https://orcid.org/0000-0001-7309-4229
Jiliang Qiu
https://orcid.org/0000-0001-6541-515X
Ting Pang
https://orcid.org/0000-0003-1437-7442
Lin Huang
https://orcid.org/0000-0002-4899-9621
Xuexia Zhang
https://orcid.org/0000-0002-5031-8936

ABSTRACT

Purpose: Four and a half LIM protein 1 (FHL1) is involved in breast cancer (BC) development, but the regulatory mechanism involved remain unclear. In the present study, we examined the role of FHL1 in BC development.
Methods: The expression of FHL1, miR-183-5p, and miR-96-5p in BC tissues was analyzed using StarBase analysis. FHL1 expression in BC tissues, a normal human breast epithelial cell line, and BC cell lines was detected using quantitative reverse transcription polymerase chain reaction (qRT-PCR). The relationship between FHL1 and miR-183-5p/miR-96-5p was analyzed via Pearson's rank correlation, TargetScan, and a dual-luciferase reporter assay. BT549 and MDA-MB-231 cells were transfected with either FHL1 and miR-183-5p mimics, or siFHL1 and a miR-183-5p inhibitor, respectively. The viability, colony number, migration, invasion, and tube length of BT549 and MDA-MB-231 cells were examined using cell counting kit-8, colony formation, wound-healing, Transwell, and tube formation assays, respectively. The levels of FHL1, vascular endothelial growth factor (VEGF), p53, E-cadherin, N-cadherin, and vimentin were quantified using western blotting and qRT-PCR.
Results: FHL1 expression was downregulated in BC tissues and cells, whereas miR-183-5p and miR-96-5p were upregulated in BC tissues (negative correlation with FHL1 expression). FHL1 overexpression inhibited the viability, colony number, migration, and invasion of BC cells and the expression of VEGF, N-cadherin, and vimentin, and increased the expression of FHL1, p53, and E-cadherin in BT549 cells. Furthermore, a miR-183-5p mimic reversed these effects of FHL1 overexpression, whereas FHL1 silencing caused opposite results to those observed in MDA-MB-231 cells; however, this was reversed by a miR-183-5p inhibitor.
Conclusion: Our study suggests that miR-183-5p promotes cell proliferation, metastasis, and angiogenesis by negatively regulating FHL1 in BC.

Keywords: Breast neoplasms; FHL1 protein, human; MicroRNAs; Neoplasm metastasis

Conflict of Interest
The authors declare that they have no competing interests.

Author Contributions
Conceptualization: Li Y, Zeng Q; Data curation: Zeng Q, Huang L; Formal analysis: Li Y, Qiu J; Investigation: Pang T; Methodology: Qiu J, Pang T, Zhang X; Project administration: Qiu J, Huang L; Software: Zhang X; Validation: Pang T; Visualization: Zhang X; Writing - original draft: Li Y, Zeng Q.

INTRODUCTION

Driven by many genetic or epigenetic alterations and molecular events, breast cancer (BC) is a molecularly heterogeneous disease that represents the most frequent malignant tumor in women and is a predominant cause of tumor-associated mortality worldwide [1]. Metastasis imposes substantial difficulties on the treatment of patients with BC [2]. The survival rate of patients with BC is still low despite the constant development of modern treatments [2,3]. Blood vessels provide tumors with nutrition and oxygen used for growing into a solid tumor [4], and angiogenesis is a precondition for tumor growth and metastasis [5]. Therefore, the identification of novel cancer markers and the potential molecular mechanisms of metastasis and angiogenesis of BC is urgently needed.

Four and a half LIM protein 1 (FHL1), which has been identified as a tumor suppressor gene in multiple malignancies [6-8], suppresses the growth of tongue squamous cell carcinoma cells through G1/S cell cycle arrest [7]. FHL1 silencing promotes the growth of HepG2 and HeLa cells [8]. Low expression of FHL1 is speculated to play a role in the development and progression of lung cancer [6]. Moreover, Qin et al. [9] suggested that low expression of FHL1 is closely correlated to tumor invasion and metastasis of BC. Additionally, FHL1 modulates BC cell growth [10]. However, the exact role(s) of FHL1 in the metastasis and angiogenesis of BC remains unclear.

MicroRNAs (miRNAs) inhibit protein translation by targeting the 3′-untranslated region (3′-UTR) of target messenger RNAs (mRNAs) [11]. Recently, differentially expressed miRNAs in cancer cells have been reported to be closely associated with tumor occurrence and development [12,13]. Differentially expressed miRNAs in BC often play an important role in BC development by binding to their target mRNAs [14]. Shi et al. [15] reported that miR-96-5p plays a role in the development of BC and therefore could be used as an anti-cancer drug for improving BC treatment. Cheng et al. [14] demonstrated that miR-183-5p enhances cell proliferation and suppresses apoptosis of human BC cells by regulating programmed cell death protein 4, which might be a potential therapeutic target for patients with BC. Our study explored the relationship between FHL1 and miR-183-5p/miR-96-5p, and the role of the interaction between FHL1 and miR-183-5p in the proliferation, metastasis, and angiogenesis of BC.

METHODS

Clinical specimens

Fifty pairs of BC tissues and neighboring non-tumor breast tissues were collected from patients diagnosed with triple-negative BC (TNBC) at The Fifth Affiliated Hospital, Sun Yat-sen University, between June 2017 and July 2018. All these patients underwent surgery and did not undergo radiotherapy or chemotherapy prior to the study. Signed informed consent was obtained before surgery. The current experiment was approved by the Ethics Committee of The Fifth Affiliated Hospital, Sun Yat-sen University (approval number: SY2017040212).

Cell culture

A normal human breast epithelial cell line (MCF-10A) and BC cell lines (SK-BR-3, BT549, MCF7, MDA-MB-231, MDA-MB-453, and BT20) were purchased from American Tissue Culture Collection (ATCC, Manassas, USA). MCF-10A cells were cultured using the MEGM Bullet Kit (CC-3150; Lonza/Clonetics Corporation, Basel, Switzerland). SK-BR-3 cells were

https://doi.org/10.4048/jbc.2020.23.e47

cultured in McCoy's 5A Modified Medium (30-2007; ATCC). BT549 cells were cultured in Roswell Park Memorial Institute Medium 1640 (10491; Solarbio, Beijing, China). MCF7 cells were cultured in Eagle's Minimum Essential Medium (30-2003; ATCC). MDA-MB-231 and MDA-MB-453 cells were cultured in Leibovitz's L-15 Medium (30-2008; ATCC). BT20 cells were cultured in Dulbecco's Modified Eagle's Medium (DMEM, 11965; Solarbio). All culture media were supplemented with 10% fetal bovine serum (FBS, 11011-8611; Solarbio) and 1% penicillin-streptomycin liquid (P1400; Solarbio).

Cell transfection

The FHL1 sequence (GenePharma, Shanghai, China) was sub-cloned into the pcDNA3.1 vector (V79020; Thermo Fisher Scientific, Waltham, USA). siRNAs specifically targeting FHL1 (siFHL1) and siRNA negative control (siNC), miR-183-5p mimics, miR-96-5p mimics, and the miR-183-5p inhibitor were purchased from GenePharma. The scrambled RNA clone (GenePharma) with a disrupted sequence of miR-183-5p mimics or the miR-183-5p inhibitor was used as a negative control for miR-183-5p mimics and the miR-183-5p inhibitor, respectively. siNC was used as a negative control for siFHL1. The cells were transfected with different miRNAs, inhibitors, RNAs, and siRNAs for 48 hours using Lipofectamine 2000 (11668; Thermo Fisher Scientific).

Reverse transcription quantitative real-time polymerase chain reaction (PCR)

TRIzol reagent (15596018; Invitrogen, Carlsbad, USA) was used to extract total RNA. Non-miRNA genes were synthesized into cDNA via first-strand DNA synthesis (Thermo Fisher Scientific). PCR amplification was performed in a 7500 Fast Real-Time PCR System with SYBR Premix Ex Taq (Takara Biotechnology, Dalian, China). For the detection of miRNA expression, miRNAs from cultured cells were extracted using the miRNA Extraction Kit (B1802; HaiGene, Harbin, China). miRNA cDNA synthesis was performed with the HG TaqMan miRNA cDNA Synthesis Kit (B1802; HaiGene). Real-time quantitative polymerase chain reaction (qRT-PCR) analysis of miR-183-5p was performed in a 7500 Fast Real-Time PCR system using the HG TaqMan miRNA qPCR Kit (TAP02304; HaiGene). The levels of non-miRNAs and miRNAs were normalized to that of glyceraldehyde 3-phosphate dehydrogenase (GAPDH) and U6, respectively. Primers used for PCR amplification were synthesized by Sangon Biotech Co., Ltd., (Shanghai, China) and are shown in **Table 1**. Relative levels of gene expression were calculated using the $2^{-\Delta\Delta Ct}$ method [16].

Western blotting

Protein isolation from cultured cells were performed using radioimmunoprecipitation assay buffer (P0013; Beyotime, Nantong, China) with phenylmethylsulfonyl fluoride (ST506; Beyotime). Bicinchoninic acid (P0009; Beyotime) was used to determine protein concentrations. Proteins (20 μg/well) were separated on an sodium dodecyl sulfate-polyacrylamide gel electrophoresis gel and transferred onto a polyvinylidene fluoride (PVDF) membrane (IPVH00010; Millipore Corp. Bedford, USA). The PVDF membranes were washed, blocked, and incubated with primary antibodies (shown in **Table 2**) overnight at 4°C. Afterwards, the membranes were washed and incubated with a horseradish peroxidase-conjugated secondary antibody (Goat Anti-Mouse, 1:2,000, ab205719 or Goat Anti-Rabbit, 1:2,000, ab205718; both from Abcam, Cambridge, UK) at 25°C for 2 hours. Specific protein signals were developed using a luminescent image analyzer (ImageQuant LAS4000 mini; GE Healthcare, Chicago, USA) with BeyoECL Star (P0018FS; Beyotime). GAPDH was used a loading control.

https://doi.org/10.4048/jbc.2020.23.e47

Table 1. Primer sequences used for qRT-PCR

Genes	Primer sequences (5′-3′)
miR-183-5p	
forward	TATGCCACTGCTAGA ATTCACT
reverse	GTGCACGGTCCGACGT
FHL1	
forward	TGCTGCCTGAAATGCTTTGAC
reverse	GCCAGAAGCGGTTCTTATAGTG
VEGF	
forward	AGGGCAGAATCATCACGAAGT
reverse	AGGGTCTCGATTGGATGGCA
p53	
forward	CAGCACATGACGGAGGTTGT
reverse	TCATCCAAATACTCCACACGC
E-cadherin	
forward	CGAGAGCTACACGTTCACGG
reverse	GGGTGTCGAGGGAAAAATAGG
N-cadherin	
forward	TCAGGCGTCTGTAGAGGCTT
reverse	ATGCACATCCTTCGATAAGACTG
Vimentin	
forward	GACGCCATCAACACCGAGTT
reverse	CTTTGTCGTTGGTTAGCTGGT
GADPH	
forward	GGAGCGAGATCCCTCCAAAAT
reverse	GGCTGTTGTCATACTTCTCATGG
U6	
forward	CTCGCTTCGGCAGCACA
reverse	ACGCTTCACGAATTTGCGT

qRT-PCR = quantitative real-time reverse transcription polymerase chain reaction; FHL1 = four and a half LIM protein 1; VEGF = vascular endothelial growth factor; GAPDH = glyceraldehyde 3-phosphate dehydrogenase.

Table 2. List of primary antibodies used for western blots

Protein	Description	Catalog number	Company	Antibody dilution
FHL1	Rabbit	ab33912	Abcam	1:1,000
VEGF	Mouse	ab1316	Abcam	1:100
p53	Mouse	ab34712	Abcam	1:1,000
E-cadherin	Rabbit	ab40772	Abcam	1:10,000
N-cadherin	Rabbit	ab18203	Abcam	1:1,000
Vimentin	Rabbit	ab92547	Abcam	1:1,000
GAPDH	Mouse	ab8245	Abcam	1:1,000

FHL1 = four and a half LIM protein 1; VEGF = vascular endothelial growth factor; GAPDH = glyceraldehyde 3-phosphate dehydrogenase.

Cell Counting Kit (CCK)-8 assay

Cell viability was detected via CCK-8 assays (CA1210; Solarbio) according to the manufacturer's protocol. In brief, transfected cells (2×10^4 cell/well) were cultivated in 96-well plates for 48 hours. CCK-8 solution was added to the 96-well plates and cells were incubated for 4 hours. Absorbance was detected at 450 nm using a microplate reader (SpectraMax iD5; Molecular Devices, San Jose, USA).

Colony formation assay

Transfected cells (1×10^3 cells/well) were cultured in 60-mm dishes for 2 weeks at 37°C. Cells were then washed, fixed with methanol for 5 minutes, and stained with crystal violet (IC0600; Solarbio) for 3 minutes at 37°C. Colonies were counted using a microscope (Ts2r-FL; Nikon, Tokyo, Japan).

https://doi.org/10.4048/jbc.2020.23.e47

Scratch wound healing assay

Transfected cells were cultivated in 6-well plates until they reached 80%–90% confluence. After the medium was discarded, confluent cells were scratched using a 10 μL tip, washed with serum-free medium, and incubated for 24 hours. Migration was measured by counting the migrating cells under an inverted microscope at 100× magnification (Ts2r-FL; Nikon).

Transwell assay

Cells were cultivated in Transwell chambers (Corning Inc., Corning, USA) in the upper chamber with 200 μL serum-free medium, while 500 μL medium with 10% FBS was added into the lower wells. After 24 hours of culture at 37°C, non-invasive cells were gently scraped off using cotton swabs, whereas the cells adhered to the lower surface were fixed with 4% methanol for 30 minutes and stained with 0.1% crystal violet solution (IC0600; Solarbio) for 20 min at 37 °C and then photographed.

Angiogenesis assay

The BC cell culture medium was replaced by serum-free DMEM and cells were cultured for 48 h. Next, the cells were collected, centrifuged, and filtered to obtain tumor-conditioned medium. The 96-well plates were coated with 50 μL ice-cold Matrigel (Solarbio) and incubated for 30 minutes at 37°C. Then, 1×10^4 human umbilical vein endothelial cells (HUVECs) were seeded onto the gel with 200 μL tumor-conditioned medium. After incubation at 37°C for 6 hours, the tube length of HUVECs was evaluated using a 100× inverted microscope (Ts2r-FL; Nikon).

Dual-luciferase activity assay

HEK293T cells were used in a dual-luciferase activity assay. The possible target relationships between FHL1 and miR-183-5p/miR-96-5p were predicted via TargetScan. A sequence corresponding to the FHL1-3′-UTR with the predicted miR-183-5p or miR-96-5p binding site was synthesized by RiboBio Co., Ltd. (Guangzhou, China) and cloned into a luciferase reporter gene vector (E1330; Promega, Madison, USA). The sequence of the putative miR-183-5p or miR-96-5p binding site in the FHL1-3′-UTR was mutated, and FHL1-3′-UTR-mut (sequence: 5′-UGUAUUGUCCCGACUGCAAUAAA-3′) was constructed using the QuickChange Site-Directed Mutagenesis kit (Stratagene, Cedar Creek, USA). To confirm target relationships between FHL1 and miR-183-5p/miR-96-5p, HEK293T cells were cultured in 96-well plates and co-transfected either with FHL1-3′-UTR or FHL1-3′-UTR mut and a miR-183-5p mimic, or a miR-96-5p mimic by Lipofectamine 2000 (11668; Thermo Fisher Scientific). The Dual-Luciferase Reporter Assay system (E1910; Promega) was used to quantify the luciferase activity.

Statistical analysis

The data shown as mean ± standard deviation were analyzed using SPSS 19.0 software (SPSS, Inc., Chicago, USA). Significant differences between BC and normal breast samples were analyzed using StarBase. Correlation coefficients were calculated via Pearson's rank correlation. Paired *t*-tests were used for comparison of paired samples. Multiple groups were compared via one-way analysis of variance analysis. Differences were considered statistically significant when $p < 0.05$.

https://doi.org/10.4048/jbc.2020.23.e47

RESULTS

FHL1 was lowly expressed in BC tissues and cell lines

Low FHL1 expression was detected from three BC cells (basal like, HER2, luminal A, and luminal B tissues) (**Figure 1A**, $p < 0.05$). High or low expression of FHL1 was determined using the median. Based on the Gene Expression Omnibus, European Genome-Phenome Archive, and The Cancer Genome Atlas databases and Kaplan Meier plotter (http://kmplot.com/analysis/index.php?p=background), survival analysis showed that patients with high FHL1 expression had a good prognosis (**Figure 1B**, $p < 0.001$). According to qRT-PCR, FHL1 expression was lower in TNBC tissues than that in adjacent tissues (**Figure 1C**, $p < 0.001$). Except for MCF7 cells, FHL1 expression was lower in BT20, SK-BR-3, BT549, MDA-MB-231, and MDA-MB-453 cells compared to MCF-10A cells, and as it was especially low in BT549 and MDA-MB-231 cells (**Figure 1D**, $p < 0.05$ or $p < 0.01$ or $p < 0.001$), the 2 cell lines were used for subsequent experiments.

FHL1 regulated viability, migration, invasion, and tube length of BT549 and MDA-MB-231 cells

To explore the role of FHL1 in BC, siFHL1 and FHL1 were respectively transfected into BT549 and MDA-MB-231 cells to downregulate and upregulate the expression of FHL1, respectively. The results showed that siFHL1 significantly suppressed FHL1 expression in BT549 (**Figure 2A-C**, $p < 0.001$) and MDA-MB-231 cells (**Figure 2D-F**, $p < 0.001$), whereas transfection of FHL1 produced the opposite effects (**Figure 2A-F**, $p < 0.001$). FHL1 silencing significantly increased viability (**Figure 2G and H**, $p < 0.05$ or $p < 0.001$), migration (**Figure 2I-L**, $p < 0.01$ or $p < 0.001$), invasion (**Figure 3A-D**, $p < 0.001$), and tube length (**Figure 3E-F**, $p < 0.01$ or $p < 0.001$) of BT549 and MDA-MB-231 cells, whereas FHL1 overexpression produced the opposite effects (**Figure 2G-L** and **3A-F**, $p < 0.05$ or $p < 0.01$ or $p < 0.001$).

MiR-183-5p was negatively correlated with FHL1 in BC tissues and directly targeted FHL1 to downregulate its expression

As described in **Figure 4A and B**, StarBase revealed that miR-183-5p and miR-96-5p were upregulated in BC tissues compared to adjacent normal tissues. Moreover, miR-183-5p expression was negatively correlated with the expression of FHL1 in BC tissues (**Figure 4C**, $p < 0.001$), and miR-96-5p expression was also negatively correlated with the expression of FHL1 in BC tissues (**Figure 4D**, $p < 0.001$). We predicted a relationship between FHL1 and miR-183-5p/miR-96-5p using TargetScan, and found that miR-183-5p (**Figure 4E**) and miR-96-5p (**Figure 4F**) could bind to the FHL1-3′-UTR. Dual-luciferase reporter assays revealed that miR-183-5p mimics decreased the luciferase activity associated with the FHL1-3′-UTR compared to the Control + FHL1-3′-UTR group (**Figure 4G**, $p < 0.001$), but did not change the luciferase activity of the FHL1-3′-UTR mut (**Figure 4G**). However, miR-96-5p did not affect the luciferase activities of FHL1-3′-UTR and FHL1-3′-UTR mut (**Figure 4H**).

miR-183-5p overexpression stimulated proliferation, migration, invasion, and tube length of BT549 cells, effects which were partially reversed by FHL1 overexpression

To explore the interaction between FHL1 and miR-183-5p in BC, BT549 cells were transfected with FHL1 and a miR-183-5p mimic to upregulate the expression of FHL1 and miR-183-5p. qRT-PCR analyses showed that the miR-183-5p mimic significantly increased miR-183-5p expression in BT549 cells (**Figure 5A**, $p < 0.001$). As shown in **Figure 5B**, FHL1 transfection did not alter miR-183-5p expression or reverse the effect of the miR-183-5p mimic on miR-183-5p expression.

https://doi.org/10.4048/jbc.2020.23.e47

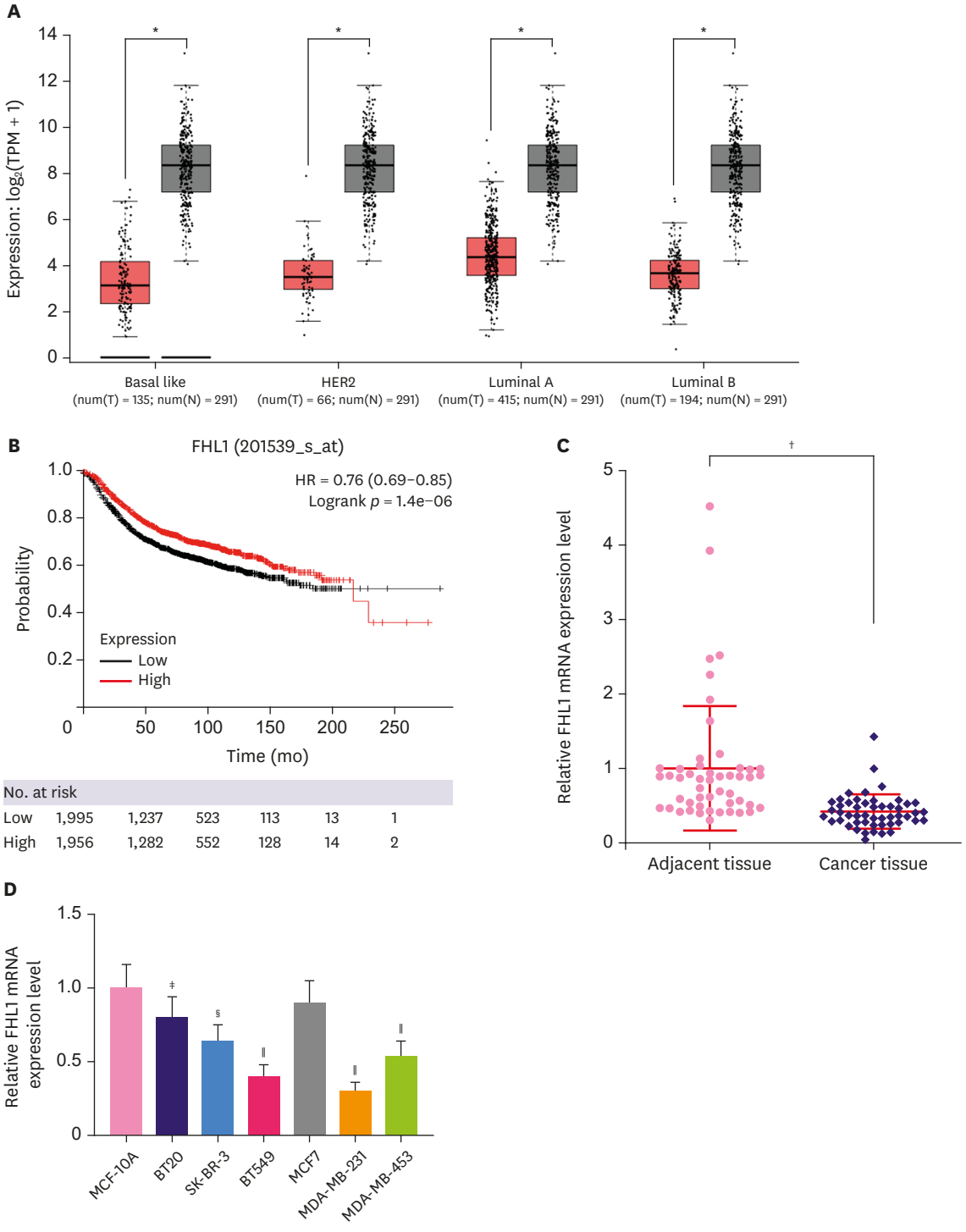

Figure 1. FHL1 expression was downregulated in several BC tissues and BC cell lines. (A) FHL1 expression in various BC tissues was analyzed via StarBase. (B) A Kaplan-Meier plotter was used to analyze the correlation between FHL1 expression and survival rate of patients with BC. (C) FHL1 expression in TNBC tissues and adjacent breast tissues was determined using qRT-PCR. (D) FHL1 expression in the normal human breast epithelial cell line MCF-10A and human BC cell lines (SK-BR-3, BT549, MCF7, MDA-MB-231, and MDA-MB-453) was determined using qRT-PCR. GAPDH was used as an internal control. The data are shown as mean ± standard deviation.

BC = breast cancer; FHL1 = four and a half LIM protein 1; TNBC = triple-negative breast cancer; qRT-PCR = quantitative real-time reverse transcription polymerase chain reaction; GAPDH = glyceraldehyde 3-phosphate dehydrogenase.

$^{*}p < 0.5$ or $^{\dagger}p < 0.001$ vs. cancer tissue. $^{\ddagger}p < 0.5$ or $^{\S}p < 0.01$ or $^{\|}p < 0.001$ vs. MCF-10A.

https://doi.org/10.4048/jbc.2020.23.e47

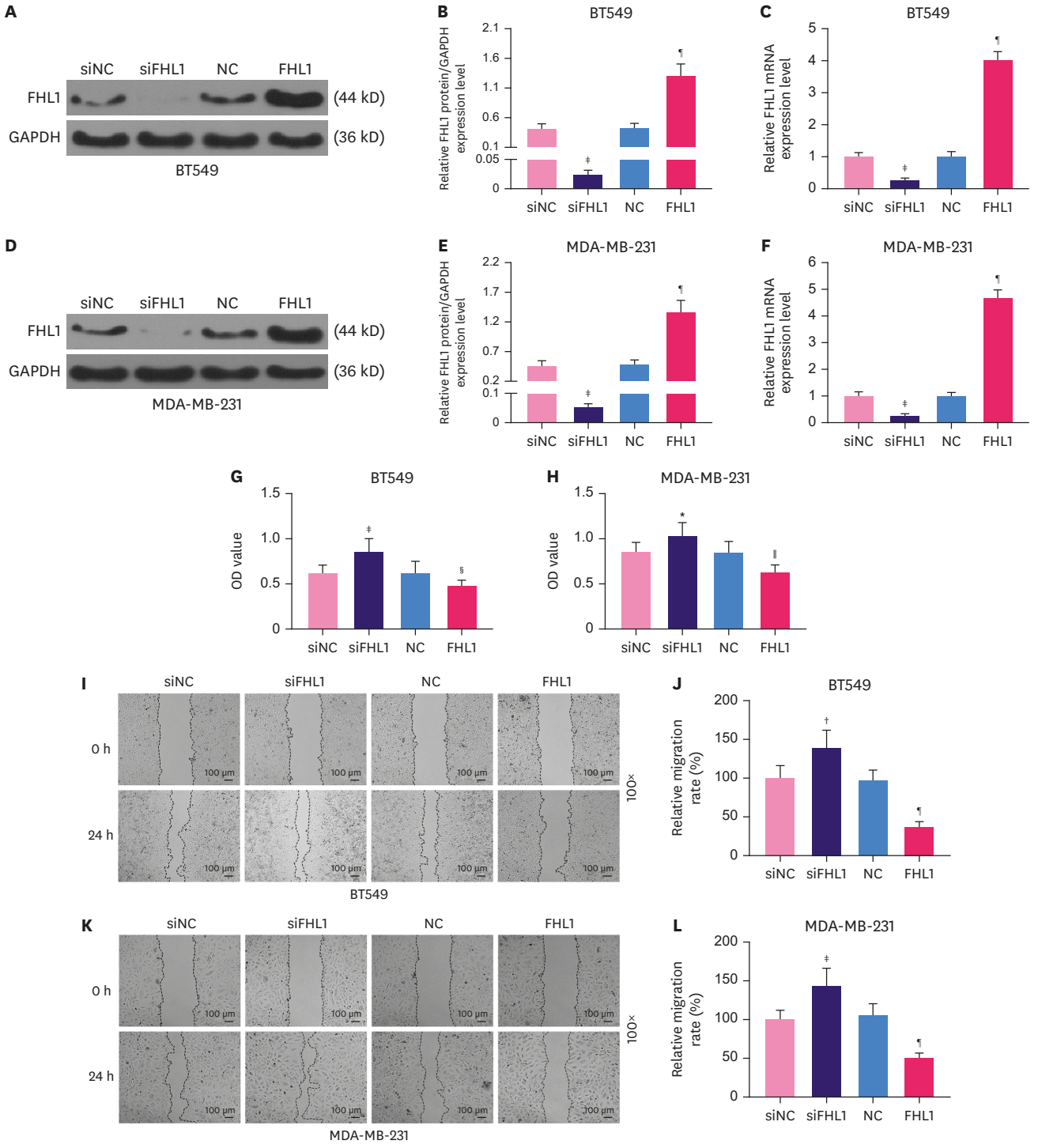

Figure 2. The transfection of FHL1 or siFHL1 regulated FHL1 expression, viability, and migration of BT549 and MDA-MB-231 cells. (A and B) FHL1 protein expression in BT549 cells transfected with siFHL1 or FHL1 was determined via western blotting. (C) FHL1 mRNA expression in BT549 cells transfected with siFHL1 or FHL1 was determined using qRT-PCR. (D and E) FHL1 protein expression in MDA-MB-231 cells transfected with siFHL1 or FHL1 was determined using western blotting. (F) FHL1 mRNA expression in MDA-MB-231 cells transfected with siFHL1 or FHL1 was determined using qRT-PCR. (G) The viability of BT549 cells transfected with siFHL1 or FHL1 was determined using a CCK-8 assay. (H) The viability of MDA-MB-231 cells transfected with siFHL1 or FHL1 was determined using a CCK-8 assay. (I) Migration of BT549 cells transfected with siFHL1 or FHL1 was determined using a scratch assay. (K) Migration of MDA-MB-231 cells transfected with siFHL1 or FHL1 was determined using a scratch assay. GAPDH was used as an internal control. The data are shown as mean ± standard deviation.
FHL1 = four and a half LIM protein 1; siFHL1 = siRNAs specifically targeting FHL1; qRT-PCR = quantitative real-time reverse transcription polymerase chain reaction; mRNA = messenger RNA; CCK = Cell Counting Kit; GAPDH = glyceraldehyde 3-phosphate dehydrogenase; NC = negative control; siNC = siRNA negative control.
$^{*}p < 0.5$ or $^{\dagger}p < 0.01$ or $^{\ddagger}p < 0.001$ vs. siNC. $^{\S}p < 0.05$ or $^{\|}p < 0.001$ or $^{\P}p < 0.001$ vs. NC.

https://doi.org/10.4048/jbc.2020.23.e47

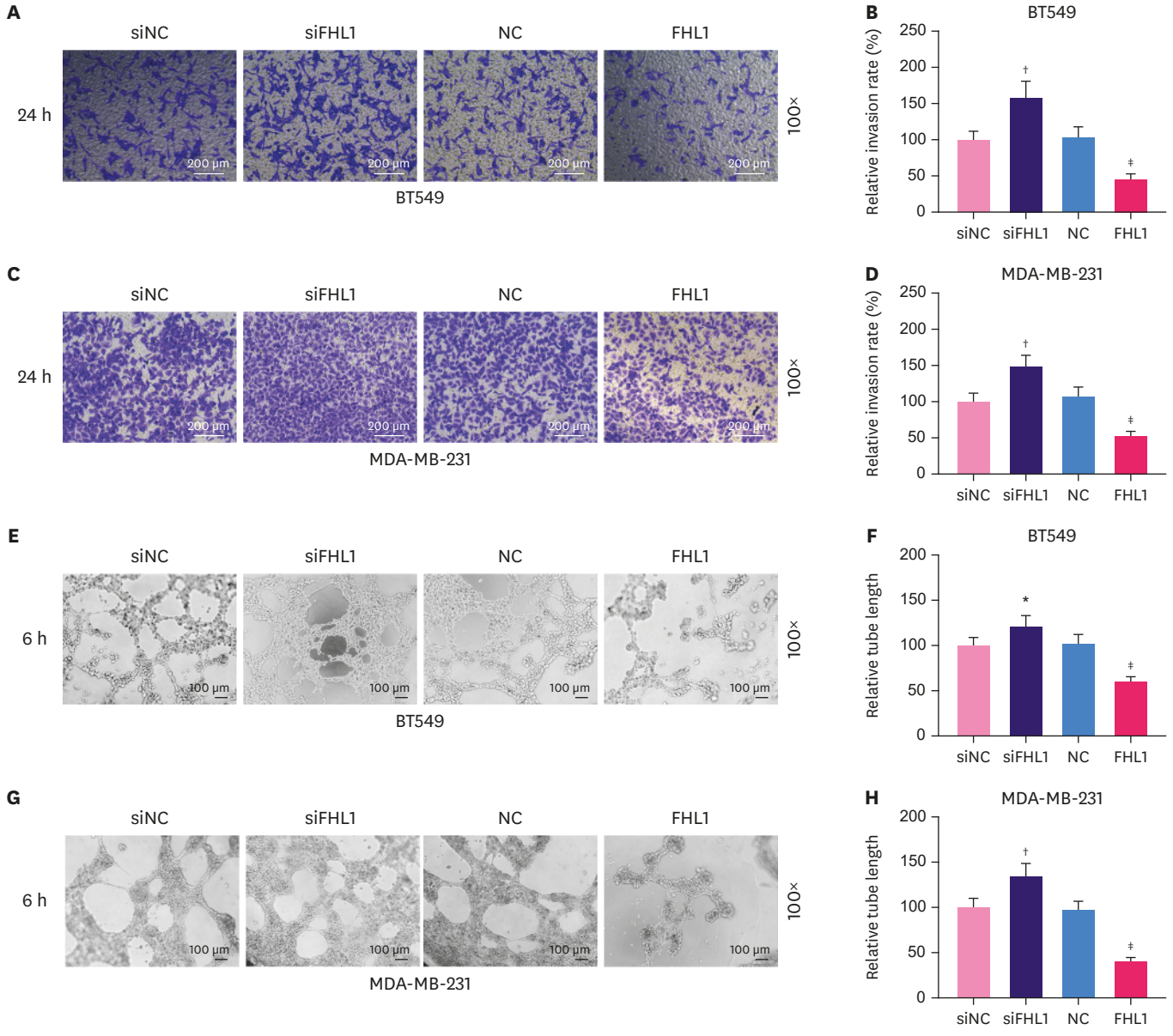

Figure 3. The transfection of FHL1 or siFHL1 regulated invasion and tube length of BT549 and MDA-MB-231 cells. (A and B) Invasion of BT549 cells transfected with siFHL1 or FHL1 was determined using a Transwell invasion assay. (C and D) The invasion rate in MDA-MB-231 cells transfected with siFHL1 or FHL1 was determined using a Transwell invasion assay. (E and F) The tube length of BT549 cells transfected with siFHL1 or FHL1 was determined using a tube formation assay. (G and H) The tube length of MDA-MB-231 cells transfected with siFHL1 or FHL1 was determined using a tube formation assay. The data are shown as mean ± standard deviation.
FHL1 = four and a half LIM protein 1; siFHL1 = siRNAs specifically targeting FHL1; NC = negative control; siNC = siRNA negative control.
*$p < 0.01$ or †$p < 0.001$ vs. siNC. ‡$p < 0.001$ vs. NC.

In addition, miR-183-5p overexpression significantly increased the viability (**Figure 5C**, $p < 0.001$), colony number (**Figure 5D and E**, $p < 0.001$), migration (**Figure 5F and G**, $p < 0.001$), invasion (**Figure 5H and I**, $p < 0.01$), and tube length (**Figure 5J and K**, $p < 0.001$) of BC cells, phenotypes which were reversed by FHL1 overexpression (**Figure 5C-K**, $p < 0.05$ or $p < 0.001$).

The miR-183-5p mimic significantly decreased the protein expression of FHL1 (**Figure 6A and B**, $p < 0.001$), while FHL1 overexpression strongly increased the protein expression of FHL1 (**Figure 6A and B**, $p < 0.001$). This effect was partially reversed by miR-183-5p

https://doi.org/10.4048/jbc.2020.23.e47

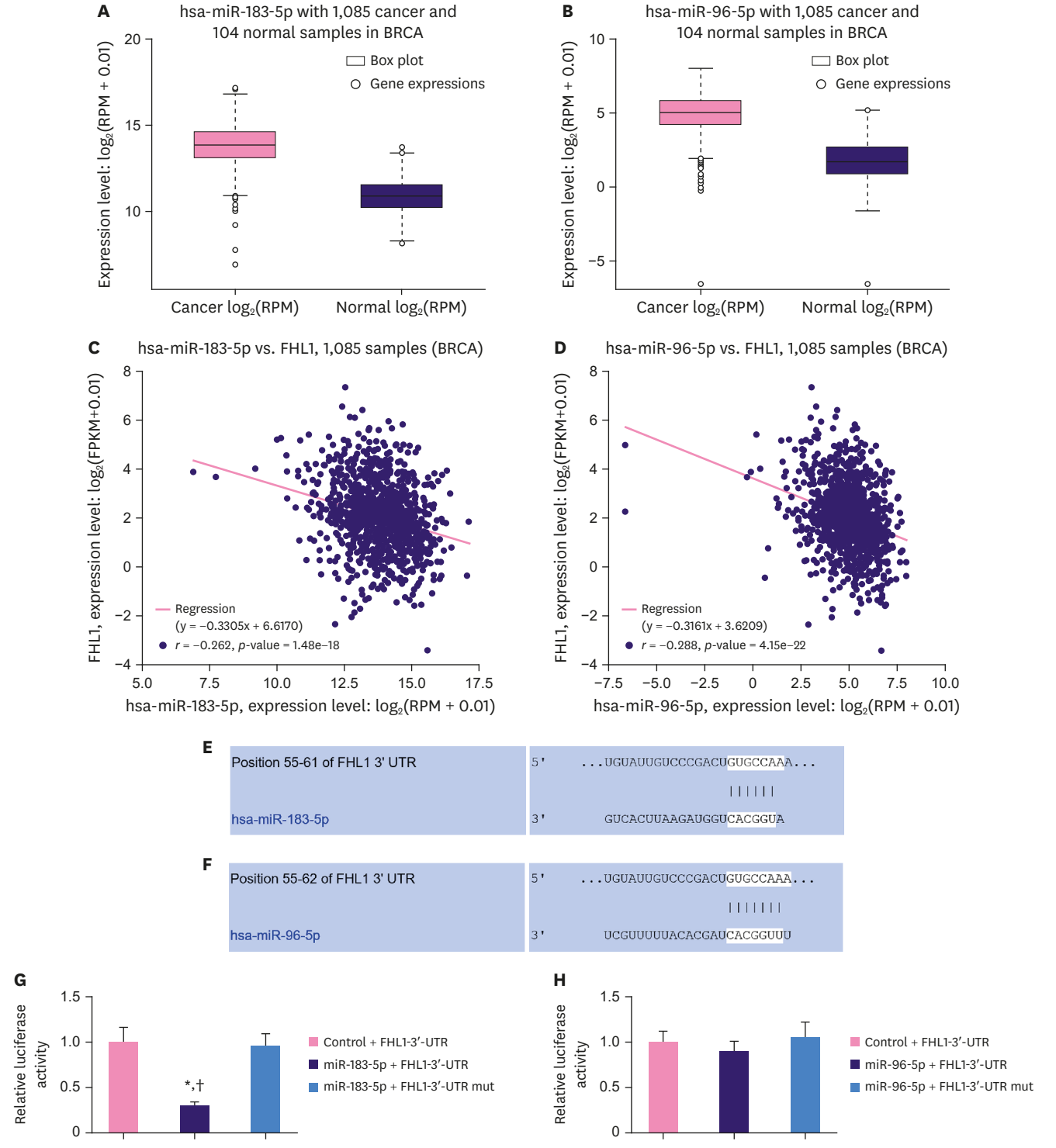

Figure 4. MiR-183-5p and miR-96-5p expression were upregulated and negatively correlated with FHL1 expression in BC tissues, and miR-183-5p directly targeted FHL1 to downregulate its expression. (A and B) MiR-183-5p and miR-96-5p expression in BC tissues were determined using StarBase. (C and D) The relationship between FHL1 and miR-183-5p/miR-96-5p was analyzed via Pearson's rank correlation. (E and F) The target relationship between FHL1 and miR-183-5p/miR-96-5p was predicted via TargetScan. (G) Luciferase activity in Control + FHL1-3′-UTR, miR-183-5p + FHL1-3′-UTR, and miR-183-5p + FHL1-3′-UTR mut groups in HEK293T cells was determined using a dual-luciferase assay. (H) Luciferase activity in Control + FHL1-3′-UTR, miR-96-5p + FHL1-3′-UTR, and miR-96-5p + FHL1-3′-UTR mut groups in HEK293T cells was determined using a dual-luciferase assay. The data are shown as mean ± standard deviation.
FHL1 = four and a half LIM protein 1; BC = breast cancer; 3′-UTR = 3′-untranslated region; mut = mutated.
*$p < 0.001$ vs. Control + FHL1-3′-UTR. †$p < 0.001$ vs. miR-183-5p + FHL1-3′-UTR mut.

https://doi.org/10.4048/jbc.2020.23.e47

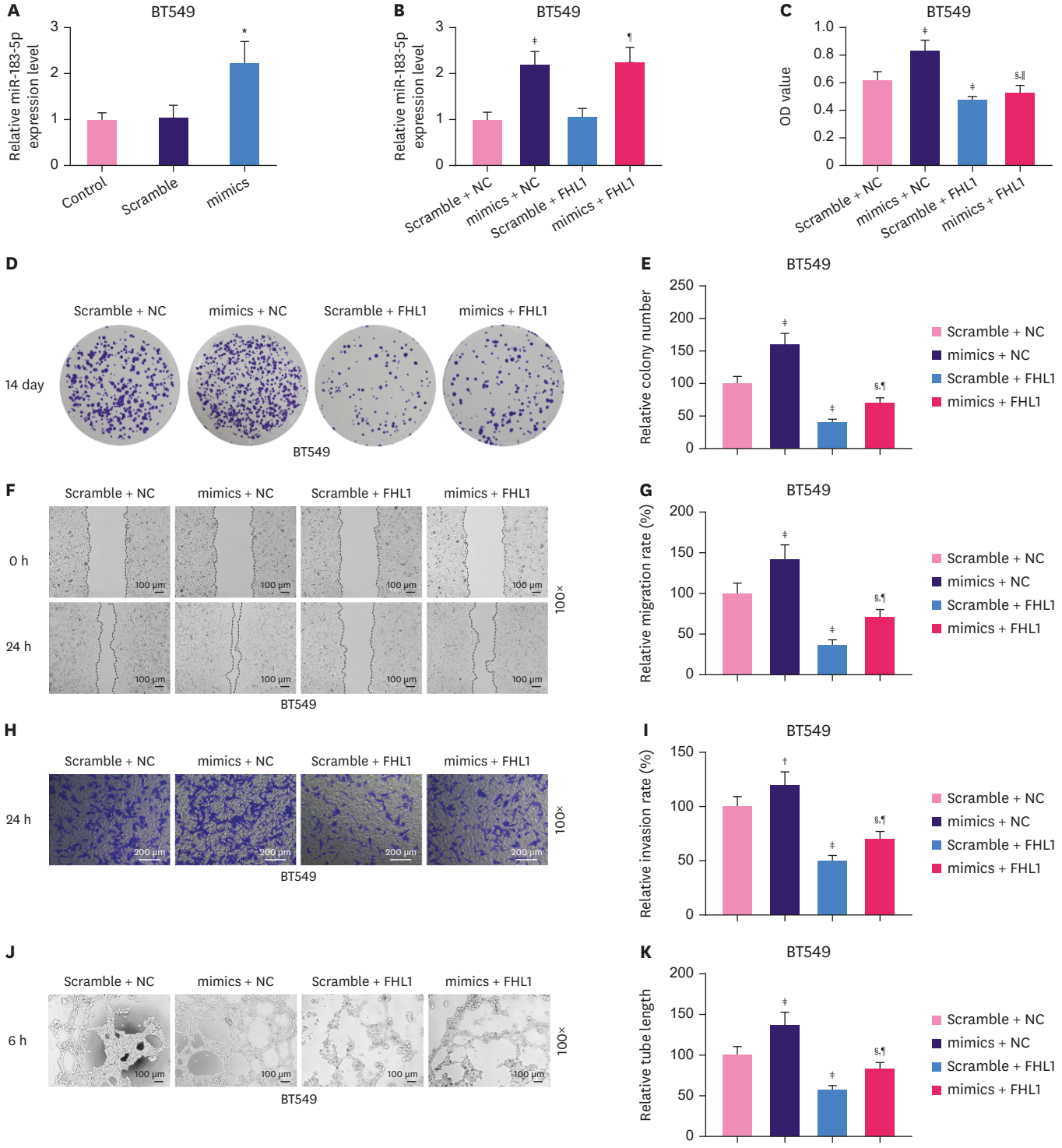

Figure 5. miR-183-5p overexpression stimulated the proliferation, migration, invasion, and tube length of BT549 cells, which were partially reversed by FHL1 overexpression. (A) miR-183-5p expression in BT549 cells transfected with miR-183-5p mimics was quantified using qRT-PCR. (B) miR-183-5p expression in BT549 cells transfected with miR-183-5p mimics or FHL1 or co-transfected with miR-183-5p mimics and FHL1 was quantified using qRT-PCR. Viability (C), colony number (D and E), migration (F and G), invasion (H and I), and tube length (J and K) of BT549 cells transfected with miR-183-5p mimics or FHL1 or co-transfected with miR-183-5p mimics and FHL1 were measured using CCK-8, colony formation, scratch wound-healing, Transwell invasion, and tube formation assays, respectively. U6 was used as an internal control. The scramble NC is a disrupted sequence of miR-183-5p mimics. The data are shown as mean ± standard deviation.
FHL1 = four and a half LIM protein 1; qRT-PCR = quantitative real-time reverse transcription polymerase chain reaction; CCK = Cell Counting Kit; NC = negative control; OD = optical density.
*$p < 0.001$ vs. Scramble. †$p < 0.01$ or ‡$p < 0.001$ vs. Scramble + NC. §$p < 0.001$ vs. mimics + NC. ‖$p < 0.05$ or ¶$p < 0.001$ vs. Scramble + FHL1.

https://doi.org/10.4048/jbc.2020.23.e47

overexpression in BT549 cells (**Figure 6A and B**, $p < 0.001$). To further investigate the effects of the interaction between FHL1 and miR-183-5p on the migration, invasion, and tube length of BT549 cells, we quantified the expression of vascular endothelial growth factor (VEGF), p53, E-cadherin, N-cadherin, and vimentin in BT549 cells. FHL1 overexpression significantly decreased the protein expression of VEGF (**Figure 6A and C**, $p < 0.001$), but increased the expression of p53 (**Figure 6A and D**, $p < 0.001$) and E-Cadherin (**Figure 6A and E**, $p < 0.001$).

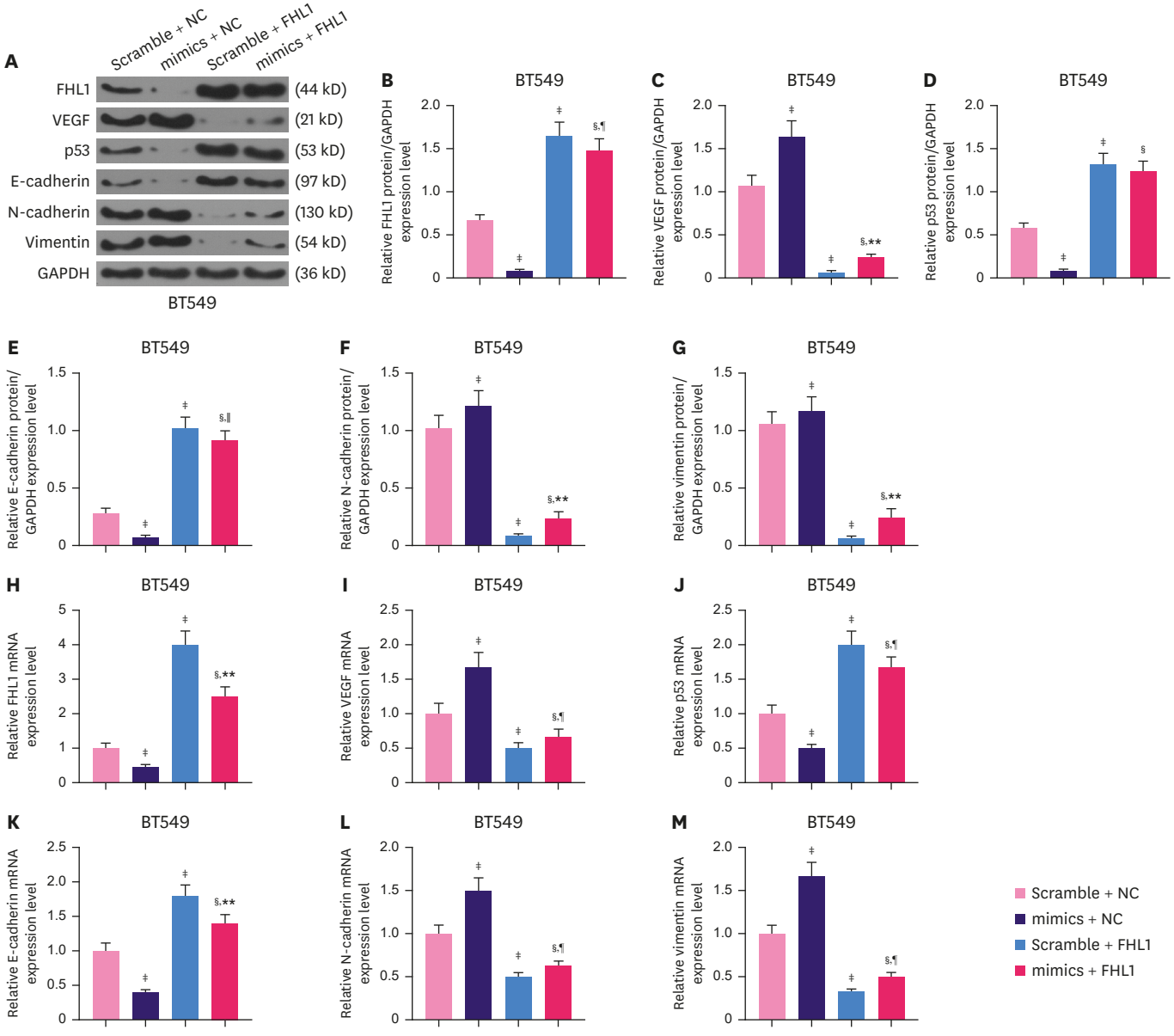

Figure 6. FHL1 overexpression partially reversed the effect of miR-183-5p overexpression on mRNA and protein levels of FHL1, VEGF, p53, E-cadherin, N-cadherin, and vimentin in BT549 cells. (A-G) The expression of FHL1, VEGF, p53, E-cadherin, N-cadherin, and vimentin proteins in BT549 cells transfected with miR-183-5p mimics or FHL1 or co-transfected with miR-183-5p mimics and FHL1 was quantified via western blotting. (H-M) The expression of FHL1, VEGF, p53, E-cadherin, N-cadherin, and vimentin mRNAs in BT549 cells transfected with miR-183-5p mimics or FHL1 or co-transfected with miR-183-5p mimics and FHL1 was quantified using qRT-PCR. GAPDH was used as an internal control. The scramble NC is a disrupted sequence of miR-183-5p mimics. The data are shown as mean ± standard deviation.
FHL1 = four and a half LIM protein 1; mRNA = messenger RNA; VEGF = vascular endothelial growth factor; qRT-PCR = quantitative real-time reverse transcription polymerase chain reaction; GAPDH = glyceraldehyde 3-phosphate dehydrogenase; NC = negative control.
$^{*}p < 0.05$ or $^{\dagger}p < 0.01$ or $^{\ddagger}p < 0.001$ vs. Scramble + NC. $^{\S}p < 0.001$ vs. mimics + NC. $^{\|}p < 0.05$ or $^{\P}p < 0.01$ or $^{**}p < 0.001$ vs. Scramble + FHL1.

https://doi.org/10.4048/jbc.2020.23.e47

The protein expression of N-Cadherin (**Figure 6A and F**, $p < 0.001$) and vimentin (**Figure 6A and G**, $p < 0.001$) was decreased by FHL1 overexpression. miR-183-5p overexpression produced the opposite effects (**Figure 6A-G**, $p < 0.05$ or $p < 0.01$ or $p < 0.001$). The effect of FHL1 overexpression on mRNA expression of FHL1, VEGF, P53, E-cadherin, N-cadherin, and Vimentin was similar to that of its protein expression (**Figure 6H-M**, $p < 0.001$), while miR-183-5p overexpression produced the opposite effects.

FHL1 silencing partially reversed the inhibitory effect of the miR-183-5p inhibitor on the proliferation, migration, invasion, and tube length of MDA-MB-231 cells

The miR-183-5p inhibitor significantly decreased miR-183-5p expression in MDA-MB-231 cells (**Figure 7A**, $p < 0.001$). Transfection with siFHL1 did not alter miR-183-5p expression or reverse the effect of the miR-183-5p inhibitor on miR-183-5p expression (**Figure 7B**). We also observed that the viability (**Figure 7C**, $p < 0.001$), colony number (**Figure 7D and E**, $p < 0.001$), migration (**Figure 7F and G**, $p < 0.001$), invasion (**Figure 7H and I**, $p < 0.001$), and tube length (**Figure 7J and K**, $p < 0.001$) of MDA-MB-231 cells were significantly decreased by low expression of miR-183-5p, and these phenotypes were completely reversed by FHL1 downregulation (**Figure 7C-K**, $p < 0.001$).

In MDA-MB-231 cells, reducing miR-183-5p expression significantly increased the proteinexpression of FHL1 (**Figure 8A and B**, $p < 0.001$), while reducing FHL1 noticeably decreased the expression of FHL1 (**Figure 8A and B**, $p < 0.001$), which was partially reversed by the low expression of miR-183-5p (**Figure 8A and B**, $p < 0.001$). The results of western blotting revealed that in MDA-MB-231 cells, low expression of FHL1 significantly elevated the expression of VEGF (**Figure 8A and C**, $p < 0.001$), but decreased p53 (**Figure 8A and D**, $p < 0.001$) and E-Cadherin (**Figure 8A and E**, $p < 0.001$), and also increased the protein expression of N-Cadherin (**Figure 8A and F**, $p < 0.001$) and vimentin (**Figure 8A and G**, $p < 0.001$), while low expression of miR-183-5p produced the opposite effects, and low expression of FHL1 can reverse the effects of the low expression of miR-183-5p (8A-G, $p < 0.001$). In addition, The effect of low expression of FHL1 on mRNA expression of FHL1, VEGF, P53, E-cadherin, N-cadherin, and Vimentin was similar to that of its protein expression (**Figure 8H-M**, $p < 0.001$), while the low expression of miR-183-5p produced the opposite effects.

DISCUSSION

FHL1 is regarded as a tumor suppressor gene and its expression is commonly downregulated in multiple malignant tumors [17]. In this study, FHL1 was found to be lowly expressed in several BC tissues, which was in accordance with the result of a previous study [9]. Additionally, our novel data further revealed that FHL1 was lowly expressed in several BC cells, which was consistent with previous findings and support that FHL1 might be a tumor suppressor gene in BC.

To confirm that FHL1 functioned as a tumor suppressor gene in BC, we primarily explored the role of FHL1 in the metastasis and angiogenesis of BC cells transfected with siFHL1 or FHL1. BC metastasis begins from local invasion, spreads into the blood or lymphatic vessels, and arrives at distal organs [2]. Cancer cell migration and invasion marks the initiation of cancer metastasis into surrounding tissue and vasculature [18]. Additionally, the sprouting of endothelial cells is the first step in tumor angiogenesis [2]. In this study, we found that

https://doi.org/10.4048/jbc.2020.23.e47

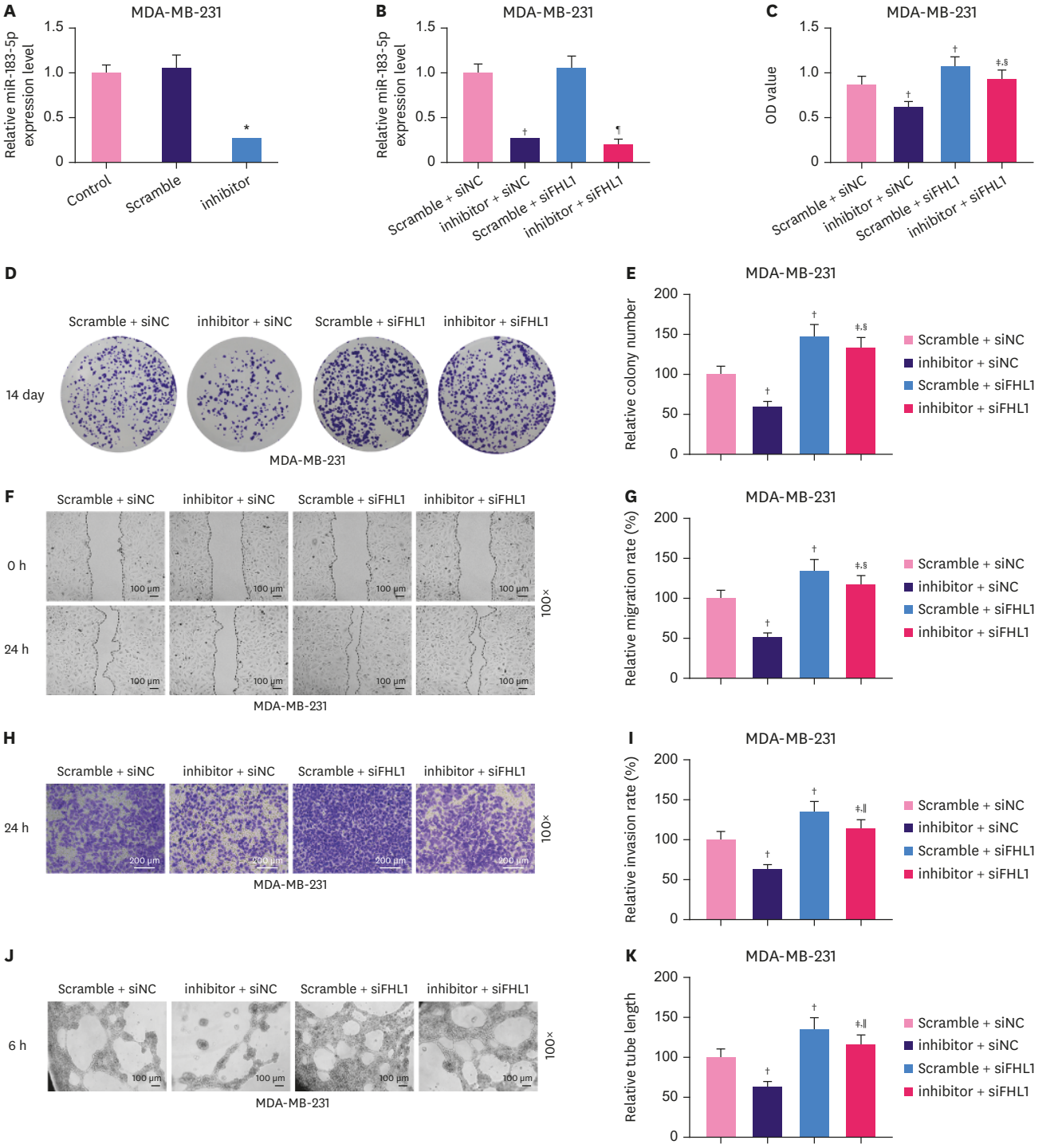

Figure 7. Low expression of FHL1 partially reversed the inhibitory effect of the low expression of miR-183-5p on the proliferation, migration, invasion, and tube length of MDA-MB-231 cells. (A) MiR-183-5p expression in MDA-MB-231 cells transfected with a miR-183-5p inhibitor was quantified using qRT-PCR. (B) miR-183-5p expression in MDA-MB-231 cells transfected with a miR-183-5p inhibitor or siFHL1 or co-transfected with miR-183-5p inhibitor and siFHL1 was quantified using qRT-PCR. Viability (C), colony number (D and E), migration rate (F and G), invasion rate (H and I), and tube length (J and K) of MDA-MB-231 cells transfected with a miR-183-5p inhibitor or siFHL1 or co-transfected with a miR-183-5p inhibitor and siFHL1 was measured using CCK-8, colony formation, scratch wounding-healing, Transwell invasion, and tube formation assays, respectively. U6 was used as an internal control. The scramble NC is a disrupted sequence of the miR-183-5p inhibitor. The data are shown as mean ± standard deviation.
FHL1 = four and a half LIM protein 1; qRT-PCR = quantitative real-time reverse transcription polymerase chain reaction; siFHL1 = siRNAs specifically targeting FHL1; CCK = Cell Counting Kit; NC = negative control.
*$p < 0.001$ vs. Scramble. †$p < 0.001$ vs. Scramble + siNC. ‡$p < 0.001$ vs. inhibitor + siNC. §$p < 0.05$ or ‖$p < 0.01$ or ¶$p < 0.001$ vs. Scramble + siFHL1.

https://doi.org/10.4048/jbc.2020.23.e47

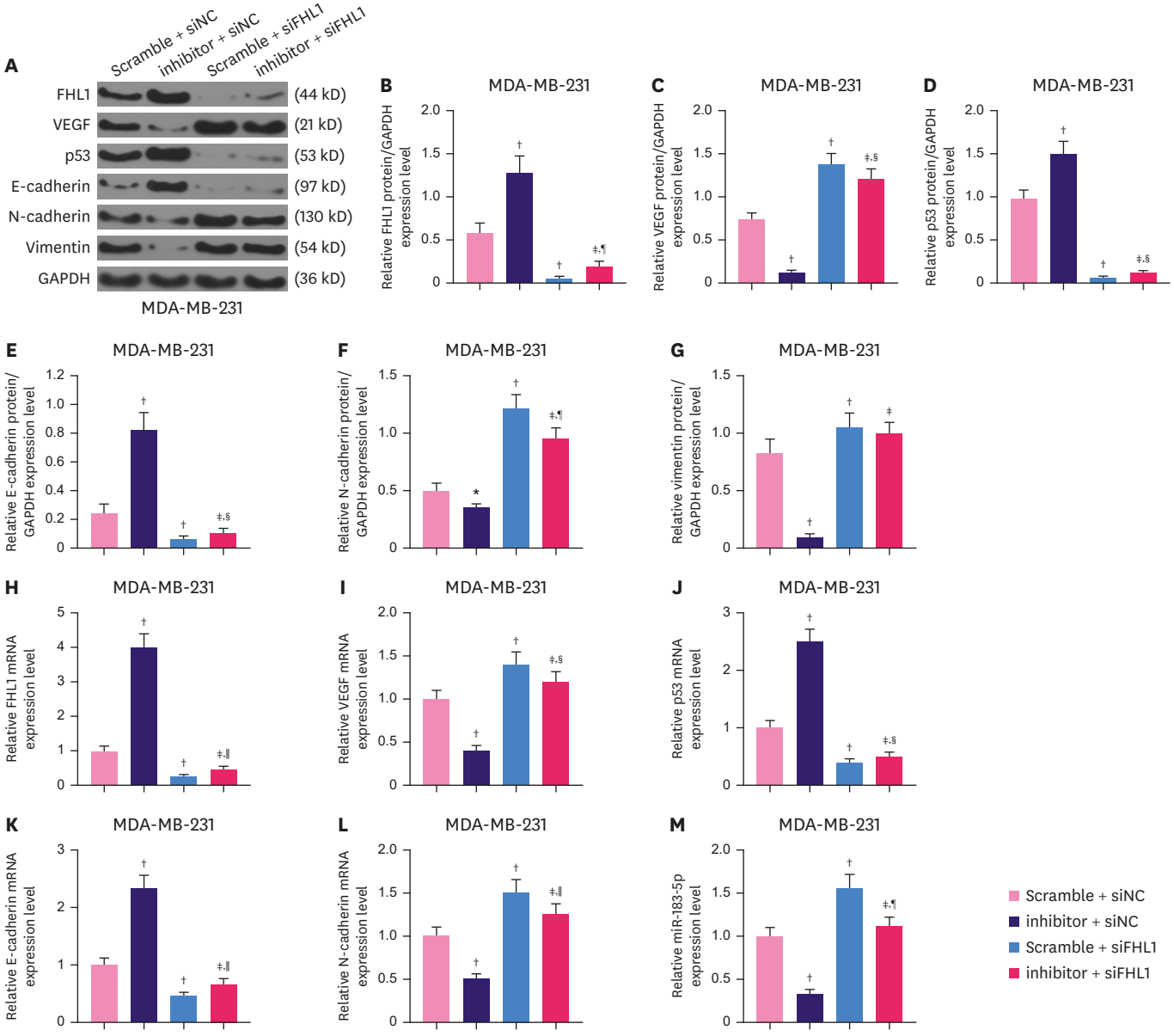

Figure 8. Low expression of FHL1 partially reversed the effect of miR-183-5p downregulation on the expressions of FHL1, VEGF, p53, E-cadherin, N-cadherin, and vimentin mRNAs and the protein in MDA-MB-231 cells. (A-G) The levels of FHL1, VEGF, p53, E-cadherin, N-cadherin, and vimentin protein in MDA-MB-231 cells transfected with a miR-183-5p inhibitor or siFHL1 or co-transfected with a miR-183-5p inhibitor and siFHL1 were determined using western blotting. (H-M) The levels of FHL1, VEGF, p53, E-cadherin, N-cadherin, and vimentin mRNAs in MDA-MB-231 cells transfected with a miR-183-5p inhibitor or siFHL1 or co-transfected with a miR-183-5p inhibitor and siFHL1 were quantified via qRT-PCR. GAPDH was used as an internal control. The scramble negative control is disrupted sequence of the miR-183-5p inhibitor. The data are shown as mean ± standard deviation.
FHL1 = four and a half LIM protein 1; VEGF = vascular endothelial growth factor; siFHL1 = siRNAs specifically targeting FHL1; qRT-PCR = quantitative real-time reverse transcription polymerase chain reaction.
$^{*}p < 0.01$ or $^{\dagger}p < 0.001$ vs. Scramble + siNC. $^{\ddagger}p < 0.001$ vs. inhibitor + siNC. $^{\S}p < 0.05$ or $^{\|}p < 0.01$ or $^{\P}p < 0.001$ vs. Scramble + siFHL1.

FHL1 overexpression suppressed the viability, migration, invasion, and tube formation of BC cells, whereas FHL1 silencing produced the opposite effects. These data suggest that FHL1 functions as a tumor suppressor in the development of BC.

Differentially expressed miRNAs can regulate the same mRNA [19]. Wang et al. [20] demonstrated that miR-410 is highly expressed in liver and colorectal tumors, and promotes

https://doi.org/10.4048/jbc.2020.23.e47

tumor cell growth by negatively regulating FHL1. However, the effect of FHL1 regulation on BC has not been reported. In the present study, high expression of miR-183-5p and miR-96-5p were detected in BC tissues, and their expression was negatively correlated with FHL1 expression, indicating that FHL1 might be modulated by miR-183-5p and miR-96-5p. According to TargetScan, both miR-183-5p and miR-96-5p share a binding site in FHL1. However, the results of the dual-luciferase activity revealed that only miR-183-5p can regulate FHL1. These results confirmed that FHL1 was a target of miR-183-5p.

Previous studies have reported that miRNAs regulate the migration and invasion of different cancers, necessitating the characterization of their functions [21]. Moreover, studies have reported that miR-183-5p executes important functions in multiple tumors. In human endometrial cancer cells, miR-183-5p overexpression inhibits the proliferation, invasion, migration, and epithelial to mesenchymal transition (EMT) [22]. Wang et al. [23] demonstrated that miR-183-5p promotes tumor growth and metastasis of lung cancer cells *in vivo*. EMT is a process through which epithelial cells are transformed into mesenchymal cells, and is associated with cancer cell migration and invasion as a result of loss of cell-cell adhesion. Therefore, EMT plays a pivotal role in the metastasis of cancer cells [24]. EMT is a feature of aggressive tumors, and is characterized by decreased E-cadherin and increased N-cadherin expression [25]. Vimentin is an EMT marker, is ubiquitously expressed in normal mesenchymal cells, and maintains cellular integrity [26]. Additionally, it has been reported that miRNA dysregulation is involved in angiogenesis, and miRNAs may induce tumorigenesis by affecting the production of angiogenic factors and neovascularization [27]. Excessive tumor growth stimulates the formation of new blood vessels to sustain its growth, which begins with the acceleration of protein synthesis, including the synthesis of VEGF [28]. VEGF is a key angiogenic mediator that has broad effects on the development and maintenance of abnormal tumor vasculature [29]. As an important tumor suppressor gene, p53 inhibits VEGF expression, tumor growth, and metastasis [30]. In the present study, miR-183-5p overexpression was observed to promote the viability, colony number, migration, invasion, and tube length of the BT549 cells, and the expression of VEGF, N-cadherin, and vimentin, but suppressed the expression of p53 and E-cadherin through inhibition of FHL1 expression. In contrast, lowly expressed miR-183-5p produced the opposite effects by increasing FHL1 expression in MDA-MB cells.

Therefore, these data revealed that miR-183-5p promotes the proliferation, metastasis, and angiogenesis of BC cells by increasing the expression of VEGF, N-cadherin, and vimentin, and inhibiting the expression of p53 and E-cadherin by inhibiting FHL1 expression in BC.

Taken together, the present results demonstrated that FHL1 is a target gene of miR-183-5p, and their expression is negatively correlated in BC. MiR-183-5p reversed the inhibitory effect of FHL1 on the proliferation, metastasis, and angiogenesis of BC cells. The current results suggest a novel potential mechanism underlying BC progression, which will contribute to advancing BC treatment.

REFERENCES

1. Wörmann B. Breast cancer: basics, screening, diagnostics and treatment. Med Monatsschr Pharm 2017;40:55-64.
PUBMED

2. McGuire A, Brown JA, Kerin MJ. Metastatic breast cancer: the potential of miRNA for diagnosis and treatment monitoring. Cancer Metastasis Rev 2015;34:145-55.
PUBMED | CROSSREF
3. Xu Y, Liu Z, Guo K. Expression of FHL1 in gastric cancer tissue and its correlation with the invasion and metastasis of gastric cancer. Mol Cell Biochem 2012;363:93-9.
PUBMED | CROSSREF
4. Warren BA, Shubik P. The growth of the blood supply to melanoma transplants in the hamster cheek pouch. Lab Invest 1966;15:464-78.
PUBMED
5. Weidner N, Carroll PR, Flax J, Blumenfeld W, Folkman J. Tumor angiogenesis correlates with metastasis in invasive prostate carcinoma. Am J Pathol 1993;143:401-9.
PUBMED
6. Niu C, Liang C, Guo J, Cheng L, Zhang H, Qin X, et al. Downregulation and growth inhibitory role of FHL1 in lung cancer. Int J Cancer 2012;130:2549-56.
PUBMED | CROSSREF
7. Ren W, Lian P, Cheng L, Du P, Guan X, Wang H, et al. FHL1 inhibits the growth of tongue squamous cell carcinoma cells via G1/S cell cycle arrest. Mol Med Rep 2015;12:3958-64.
PUBMED | CROSSREF
8. Fan Z, Xu X, Zhang X, Wang T, Han B, Liang Y, et al. FHL1 knockdown mediated by lentiviral shRNA promotes the growth of HeLa and HepG2 cells. Xibao Yu Fenzi Mianyixue Zazhi 2015;31:879-83.
PUBMED
9. Qin WX, Yan F, Wang YJ. Expressions of KISS1, KAI1 and FHL1 and neoplasms metastasis. J Clin Med Pract 2010;14:37-40.
CROSSREF
10. Ding L, Niu C, Zheng Y, Xiong Z, Liu Y, Lin J, et al. FHL1 interacts with oestrogen receptors and regulates breast cancer cell growth. J Cell Mol Med 2011;15:72-85.
PUBMED | CROSSREF
11. De Los Reyes-García AM, Arroyo AB, Teruel-Montoya R, Vicente V, Lozano ML, González-Conejero R, et al. MicroRNAs as potential regulators of platelet function and bleeding diatheses. Platelets 2019;30:803-8.
PUBMED | CROSSREF
12. Chen F, Li XF, Fu DS, Huang JG, Yang SE. Clinical potential of miRNA-221 as a novel prognostic biomarker for hepatocellular carcinoma. Cancer Biomark 2017;18:209-14.
PUBMED | CROSSREF
13. Zhou Y, Ren H, Dai B, Li J, Shang L, Huang J, et al. Hepatocellular carcinoma-derived exosomal miRNA-21 contributes to tumor progression by converting hepatocyte stellate cells to cancer-associated fibroblasts. J Exp Clin Cancer Res 2018;37:324.
PUBMED | CROSSREF
14. Cheng Y, Xiang G, Meng Y, Dong R. MiRNA-183-5p promotes cell proliferation and inhibits apoptosis in human breast cancer by targeting the PDCD4. Reprod Biol 2016;16:225-33.
PUBMED | CROSSREF
15. Shi Y, Zhao Y, Shao N, Ye R, Lin Y, Zhang N, et al. Overexpression of microRNA-96-5p inhibits autophagy and apoptosis and enhances the proliferation, migration and invasiveness of human breast cancer cells. Oncol Lett 2017;13:4402-12.
PUBMED | CROSSREF
16. Livak KJ, Schmittgen TD. Analysis of relative gene expression data using real-time quantitative PCR and the $2^{-\Delta\Delta CT}$ method. Methods 2001;25:402-8.
PUBMED | CROSSREF
17. Wang J, Huang F, Huang J, Kong J, Liu S, Jin J. Epigenetic analysis of FHL1 tumor suppressor gene in human liver cancer. Oncol Lett 2017;14:6109-16.
PUBMED | CROSSREF
18. Duff D, Long A. Roles for RACK1 in cancer cell migration and invasion. Cell Signal 2017;35:250-5.
PUBMED | CROSSREF
19. Lu K, Wang J, Song Y, Zhao S, Liu H, Tang D, et al. miRNA-24-3p promotes cell proliferation and inhibits apoptosis in human breast cancer by targeting p27Kip1. Oncol Rep 2015;34:995-1002.
PUBMED | CROSSREF
20. Wang Y, Fu J, Jiang M, Zhang X, Cheng L, Xu X, et al. MiR-410 is overexpressed in liver and colorectal tumors and enhances tumor cell growth by silencing FHL1 via a direct/indirect mechanism. PLoS One 2014;9:e108708.
PUBMED | CROSSREF

21. Hashemi ZS, Khalili S, Forouzandeh Moghadam M, Sadroddiny E. Lung cancer and miRNAs: a possible remedy for anti-metastatic, therapeutic and diagnostic applications. Expert Rev Respir Med 2017;11:147-57.
PUBMED | CROSSREF

22. Yan H, Sun BM, Zhang YY, Li YJ, Huang CX, Feng FZ, et al. Upregulation of miR-183-5p is responsible for the promotion of apoptosis and inhibition of the epithelial-mesenchymal transition, proliferation, invasion and migration of human endometrial cancer cells by downregulating Ezrin. Int J Mol Med 2018;42:2469-80.
PUBMED | CROSSREF

23. Wang H, Ma Z, Liu X, Zhang C, Hu Y, Ding L, et al. MiR-183-5p is required for non-small cell lung cancer progression by repressing PTEN. Biomed Pharmacother 2019;111:1103-11.
PUBMED | CROSSREF

24. Tulchinsky E, Demidov O, Kriajevska M, Barlev NA, Imyanitov E. EMT: a mechanism for escape from EGFR-targeted therapy in lung cancer. Biochim Biophys Acta Rev Cancer 2019;1871:29-39.
PUBMED | CROSSREF

25. Ramamurthy VP, Ramalingam S, Gediya LK, Njar VC. The retinamide VNLG-152 inhibits f-AR/AR-V7 and MNK-eIF4E signaling pathways to suppress EMT and castration-resistant prostate cancer xenograft growth. FEBS J 2018;285:1051-63.
PUBMED | CROSSREF

26. Satelli A, Li S. Vimentin in cancer and its potential as a molecular target for cancer therapy. Cell Mol Life Sci 2011;68:3033-46.
PUBMED | CROSSREF

27. Flores-Pérez A, Marchat LA, Rodríguez-Cuevas S, Bautista-Piña V, Hidalgo-Miranda A, Ocampo EA, et al. Dual targeting of ANGPT1 and TGFBR2 genes by miR-204 controls angiogenesis in breast cancer. Sci Rep 2016;6:34504.
PUBMED | CROSSREF

28. Chandrangsu S, Sappayatosok K. p53, p63 and p73 expression and angiogenesis in keratocystic odontogenic tumors. J Clin Exp Dent 2016;8:e505-11.
PUBMED | CROSSREF

29. Drevs J. VEGF and angiogenesis: implications for breast cancer therapy. EJC Suppl 2008;6:7-13.
CROSSREF

30. Yu YF, Zhang Y, Shen N, Zhang RY, Lu XQ. Effect of VEGF, P53 and telomerase on angiogenesis of gastric carcinoma tissue. Asian Pac J Trop Med 2014;7:293-6.
PUBMED | CROSSREF